Novel di-n-butyltin(IV) derivatives: Synthesis, high levels of cytotoxicity in tumor cells and the induction of apoptosis in KB cancer cells

ARTICLE *in* EUROPEAN JOURNAL OF MEDICINAL CHEMISTRY · FEBRUARY 2012

Impact Factor: 3.45 · DOI: 10.1016/j.ejmech.2011.12.032 · Source: PubMed

3 AUTHORS, INCLUDING:

Guangya Xiang
Huazhong University of Science and Techn…

35 PUBLICATIONS **316** CITATIONS

SEE PROFILE

European Journal of Medicinal Chemistry 48 (2012) 305–312

Contents lists available at SciVerse ScienceDirect

European Journal of Medicinal Chemistry

journal homepage: http://www.elsevier.com/locate/ejmech

Original article

Novel di-n-butyltin(IV) derivatives: Synthesis, high levels of cytotoxicity in tumor cells and the induction of apoptosis in KB cancer cells

Xianmei Shang*, Nan Ding, Guangya Xiang*

Tongji School of Pharmacy, Huazhong University of Science and Technology, 13 Hangkong Road, Wuhan 430030, PR China

ARTICLE INFO

Article history:
Received 12 October 2011
Received in revised form
13 December 2011
Accepted 20 December 2011
Available online 28 December 2011

Keywords:
Organotin(IV) complex
Crystal structure
Cytotoxic activity
Apoptosis

ABSTRACT

Two classes of dibutyltin(IV) hydroxamates complexes, formulated as the mononuclear mixed-ligand diorganotin(IV) complex [$^{n}Bu_2Sn(HL)Cl$] a and the tetranuclear [$^{n}Bu_4Sn_2(HL)_2(L)]_2$ **b** were fully characterized. X-ray diffraction analyses were also carried out for the representative complexes [$^{n}Bu_2Sn$(2,6-$F_2C_6H_3C(=O)NHO)Cl$](**4a**) and [[$^{n}Bu_4Sn_2${3-$BrC_6H_4C(=O)NHO$}$_2${3-$BrC_6H_4C(=NO)O$}$]_2$](**1b**). The cytotoxicity of all compounds was tested by MTT and SRB assays against three human tumor cell lines HL-60, BGC-823 and KB. **1b** and **4a** have been shown to be more potent antitumor agents than other compounds and cisplatin. Annexin V FITC-PI assay was consistent with the MTT results. Cell cycle assay results indicated that KB cells displayed an arrest in the G_0/G_1 phase and a decrease of S phase of the cell cycle at the low concentrations of **1b**, **4a**.

1. Introduction

There have been a great number of reports highlighting the use of diorganotin(IV) complexes as antitumor agents [1–10]. Those with biologically active ligands have attracted a particular attention toward the design of potential antitumor agents. Hydroxamic acids, as inhibitors of 5-lipoxygenase, can behave as strong bidentate O-donors with bioactivity. Many organotin(IV) hydroxamates have been prepared, and some of them possess strong antitumor activity against preneoplastic rat hepatocytes (RH), Ehrlich ascites (EA), human promyelocytic leukemic (HL-60), human hepatocellular carcinoma (Bel-7402), human gastric carcinoma (BGC-823), and human nasopharyngeal carcinoma (KB) cell lines [11–19]. Among the diorganotin(IV) hydroxamates, di-n-butyltin(IV) derivatives of hydroxamic acids have received more attention due to their stronger antitumor activity than dimethyltin(IV) or diethyltin(IV) analogs.

However, their antitumor mechanisms of action are still not elucidated [20–23]. Investigations on metal-based drugs 'induction of apoptosis' have become popular with cisplatin and ruthenium compounds [24–26], suggesting that apoptosis is a possible key event in mediating the *in vitro* antitumor activity of these compounds. Inspired by the apoptosis mechanism of these metal-based antitumor complexes, we decided to check if the *in vitro* antitumor activity of dibutyltin(IV) hydroxamates complexes could relate to apoptosis by cellular biochemical studies.

Moreover, the activity of dibutyltin(IV) hydroxamate compounds is dependent on the type of molecular structure. To further explore the influence of the nature, the number and the position of the halo atom and nuclearity, in this paper, we prepared two types of dibutyltin(IV) arylhydroxamate complexes, one mononuclear chloride and the other tetranuclear, with different tin-arylhydroxamate ratios and structures, formulated as [$^{n}Bu_2Sn(HL)Cl$] **a**, [$R_4Sn_2(HL)_2(L)]_2$ **b** (Scheme 1). Only very scant information has been given [27] on these dibutyltin(IV) complexes, and the relationship between their biological activities and antitumor mechanism has not yet been investigated. In this paper, preliminary studies of antitumor activity of these complexes were carried out in three human cancer cell lines (HL-60, BGC-823 and KB). The initial mechanism of antitumor action for two compounds with high activities on KB cell line was also investigated using flow cytometry.

2. Results and discussion

2.1. Synthesis

The two classes of di-n-butyltin(IV) substituted hydroxamates [$^{n}Bu_2Sn(HL)Cl$] **a** and [$^{n}Bu_4Sn_2(HL)_2(L)]_2$ **b** were obtained by

* Corresponding authors. Tel./fax: +86 27 83692793.
E-mail addresses: shang430030@hotmail.com (X. Shang), gyxiang1968@hotmail.com (G. Xiang).

0223-5234/$ – see front matter © 2011 Elsevier Masson SAS. All rights reserved.
doi:10.1016/j.ejmech.2011.12.032

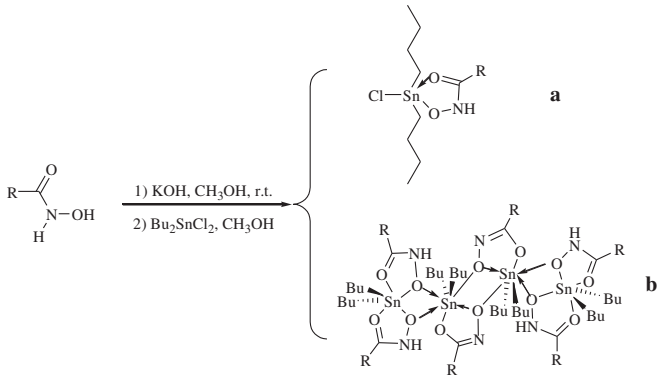

Scheme 1. Synthesis of two classes of di-n-butyltin(IV) arylhydroxamates: **a** [$^{n}Bu_2Sn(HL)Cl$] [R = 3,4-$F_2C_6H_3$ (**1a**), 2,4-$F_2C_6H_3$ (**2a**), 2,5-$F_2C_6H_3$ (**3a**), 2,6-$F_2C_6H_3$ (**4a**)] and **b** [$Bu_4Sn_2(HL)_2(L)]_2$ [R = 3-BrC_6H_4 (**1b**); 4-BrC_6H_4 (**2b**)].

reaction of the appropriate dibutyltin(IV) dichloride, in a methanol solution, with substituted hydroxamates and KOH. The complexes were isolated as white solids in moderate (27–56%) yields. They are stable in air and buffer solution. Compounds **1a**–**4a** are insoluble in water and soluble in acetone, methanol and mixtures of water/methanol, DMSO and mixtures of water/DMSO. **1b** and **2b** are also insoluble in water but soluble in chloroform, DMSO and mixtures of water/DMSO. The complexes of type **a** with chlorine atom tend to exhibit higher solubility in polar organic solvents than those of type **b**. Both complexes were characterized by FT-IR, ^{1}H, ^{13}C, ^{119}Sn NMR spectroscopies and elemental analysis. Single-crystal X-ray diffraction analyses were also carried out for the representative complexes **1b** and **4a**.

2.2. Spectroscopic data

The assignments of IR bands for all the complexes were done by comparing with the IR spectra of the free acid and related organotin(IV) compounds. The free ligand showed broad O-H absorptions in the regions of 2600–2900 cm^{-1} and 3210-3010 cm^{-1}, which were absent in the spectrum of complexes **1a**–**4a** and **1b**–**2b**, because of their deprotonation and coordination [28]. The shift towards lower frequencies of the highest (C=O) from ca. 1680 cm^{-1} in the free ligand to ca. 1620 cm^{-1} in **1a**–**4a** and **1b**–**2b** indicated that the coordination occurred through this oxygen. In the 530-410 cm^{-1} region, the two (or more) strong absorptions of **1a**–**4a** and **1b**–**2b** were assigned to the stretching mode of the Sn–O linkage [29]. The conclusions from the infrared spectra are supported by the results obtained from X-ray crystallography (see below).

The ^{1}H and ^{13}C NMR data of two complexes are given in the experimental part (from 4.2 to 4.7), and the observed resonances have been assigned on the basis of their integration and coupling constants. The ^{119}Sn NMR resonances of complexes **1a**–**4a** shows only one single around −60.3 ppm that fall within the range of pentacoordinate tin(IV) complexes [29]. For **1b** and **2b**, the chemical shifts have values −267.4, −269.7, −273.0, −279.8 ppm for **1b** and −213.2, −214.9, −215.3, −215.7 ppm for **2b**, respectively, indicating there are four tin atoms with different chemical condition belonging to the range of hexacoordinated tin atoms [30,31], as confirmed by X-ray crystal diffraction.

2.3. X-ray diffraction analysis

The crystal structure of **4a** consists of two independent complexes in the asymmetric unit with closely comparable geometries. A perspective view of the complex, together with the atom-labeling scheme, is given in Fig. 1 and selected bond angles and distances are given in the legend of Fig. 1. The coordination sphere of the tin atom is made up of two oxygen atoms, one chlorine atom and two butyl carbons, giving a pentacoordinate geometry. In the structure the 2,6-difluorobenzohydroxamato residue is a bidentate ligand, forming one short covalent and one longer coordinate oxygen-tin bond. As in other organotin hydroxamates [12,15,16,32,33], the bond lengths in the 2,6-difluorobenzohydroxamate group are consistent with a significant contribution of the zwitterionic canonical form to the electronic distribution, the C=O distance being longer and the endocyclic C–N distance shorter than normal double bond C=O and single bond C–N distance, respectively.

The heterocyclic ring is almost planar, the deviation of the Sn1 atom from the plane being 0.13 Å (0.25 Å for Sn2). The phenyl ring is rotated by 47.31° relative to the plane of the 2,6-difluorobenzohydroxamato residue. The coordination mode of the ligand produces a five-membered chelate ring with the two butyl substituents in the axial positions, which are found to be disordered owing to high thermal motion. As is to be expected, the equatorial positions are occupied by chlorine and oxygen atoms, in agreement with the polarity rule. The distortion from the ideal trigonal–bipyramidal configuration is manifested by the C(8)–Sn(1)–C(12) angle of 134.9(15)° [or C(23)–Sn(2)–C(27) angle of 141.0(11)°], which deviates from the ideal value of 180°, probably due to the ligand constraint.

The molecular structure of **1b** is shown in Fig. 2, and selected bond distances and angles are listed in the legend of Fig. 2. This structure is centrosymmetric about a $Bu_4Sn_2O_2$ core. Attached to each bridging oxygen atom is O–N=C group. Two different forms of arylhydroxamate-type ligands have been combined with the dibutyltin(IV) centers, forming six penta-membered

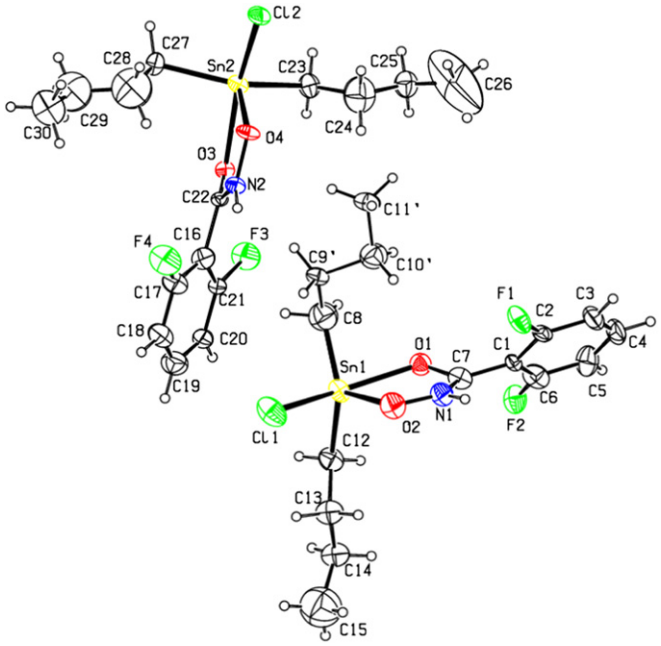

Fig. 1. Molecular structure of **4a** showing the labeling scheme of the non-H atoms. selected bond lengths (Å) and angles (○): Sn(1)–O(2) 2.15(3), Sn(1)–O(1) 2.280(19), Sn(2)–O(4) 2.018(17), Sn(2)–O(3) 2.344(14), Sn(1)–C(8) 1.96(4), Sn(1)–C(12) 2.10(3), Sn(1)–Cl(1) 2.465(9), Sn(2)–Cl(2) 2.479(7), C(7)–N(1) 1.25(4), C(7)–O(1) 1.40(3), C(22)–O(3) 1.19(3), C(22)–N(2) 1.38(3), C(8)–Sn(1)–C(12) 134.9(15), C(23)–Sn(2)–C(27) 141.0(11), C(8)–Sn(1)–Cl(1) 99.5(13), C(23)–Sn(2)–Cl(2) 101.5(8), C(12)–Sn(1)–Cl(1) 97.2(9), C(27)–Sn(2)–Cl(2) 95.3(8), O(2)–Sn(1)–Cl(1) 83.4(7), O(4)–Sn(2)–Cl(2) 82.5(4), O(1)–Sn(1)–Cl(1) 154.8(6), O(3)–Sn(2)–Cl(2) 155.8(5), O(2)–Sn(1)–O(1) 73.4(9), O(4)–Sn(2)–O(3) 73.4(6); symmetry operators: x + 1, y, z.

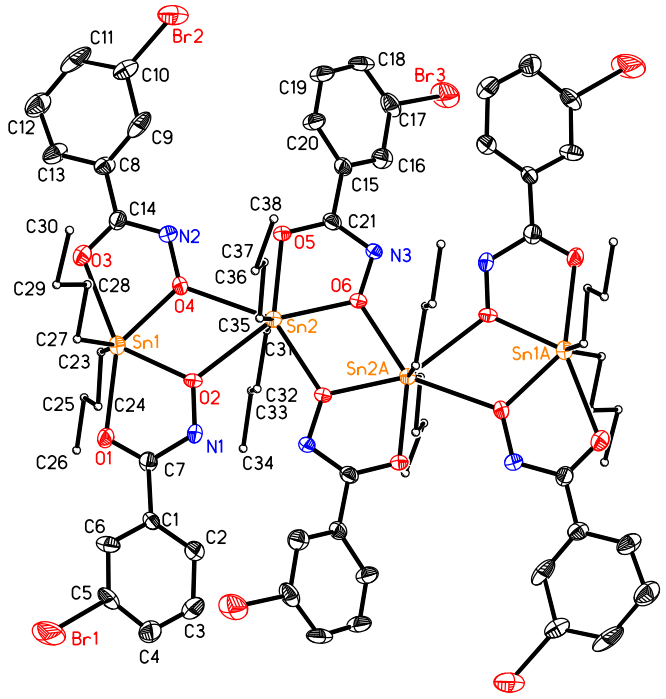

Fig. 2. Molecular structure of **1b** showing the labeling scheme of the non-H atoms. Selected bond lengths (Å) and angles (○): Sn(1)–O(2) 2.111(6), Sn(1)–O(4) 2.167(6), Sn(1)–O(1) 2.343(6), Sn(1)–O(3) 2.453(6), Sn(1)–C(23) 2.139(11), Sn(1)–C(27) 2.149(9), Sn(2)–C(31) 2.120(8), Sn(2)–C(35) 2.178(8), Sn(2)–O(5) 2.184(5), Sn(2)–O(6) 2.163(5), Sn(2)–O(2) 2.522(5), Sn(2)–O(4) 2.473(6), O(1)–C(7) 1.228(10), C(7)–N(1) 1.355(10), O(3)–C(14) 1.252(11), C(14)–N(2) 1.324(11), C(23)–Sn(1)–C(27) 141.9(5), C(21)–N(3) 1.297(10), C(31)–Sn(2)–C(35) 164.7(3), O(2)–Sn(1)–C(27) 107.7(4), O(2)–Sn(1)–O(4) 68.3(2), C(23)–Sn(1)–O(4) 103.0(4), O(2)–Sn(1)–O(1) 71.2(2), O(4)–Sn(1)–O(1) 139.3(2), O(6)–Sn(2)–C(35) 96.1(3), C(31)–Sn(2)–O(5) 87.8(3), O(6)–Sn(2)–O(5) 72.6(2), C(35)–Sn(2)–O(5) 100.4(3); symmetry operators: (A) −x + 2, −y + 2, −z + 1; (B) x, y + 1, z.

heterometallacycles. On the other hand, the hydroxamate-type ligands form two distinct groups: two of them are deprotonated at both the *N* and *O* atoms and display the hydroximic form, chelating and bridging the internal Sn2 atoms, while the other four, singly deprotonated and in the hydroxamic form, chelate the external Sn1 atoms and bridge Sn2 with Sn1. Both hydroxamate ligands at each Sn2 are almost planar. In the internal bridging hydroximate ligands, the endocyclic C(21)–N(3) and C(21)–O(5) bond lengths indicate a significant electronic delocalization in the two O–N–C–O moieties. The structure is comparable with those previously reported [15,17].

2.4. Cell-cytotoxicity assays

Two classes of dibutyltin(IV) hydroxamates compounds were evaluated for cytotoxicity *in vitro* by MTT and SRB assay against the human promyelocytic leukemic (HL-60), human gastric carcinoma (BGC-823), and human nasopharyngeal carcinoma (KB) cell lines. The screening result indicates that all organotin(IV) compounds exhibit cytotoxicities as listed in Table 1. Among all the six organotin(IV) hydroxamates, the complexes **1b** and **4a** exerted strong cytotoxic effects against tested carcinoma cell lines with a lower IC_{50} value (<1.5 μM). Compounds **1a**, **2a** and **2b** exhibited moderate inhibitory effects (IC_{50} > 2.88 μM). Moreover, almost all complexes show good selectivity against KB carcinoma cell lines. Complex **4a** with two fluorine atoms at C2 and C6 positions of benzene ring show the highest cytotoxicity against KB cell lines. It can be seen that three compounds (**1b**, **3a** and **4a**) are more active than cisplatin against KB cell lines, and **1b** and **4a** are more active than cisplatin against all tested three cell lines. Compound **4a** is better than **1b**.

Table 1
The cytotoxicity of complexes *in vitro* ($n = 5$).

Complex	IC_{50} (μM)		
	HL-60	BGC-823	KB
1a	>20	>20	15.95 ± 1.30
2a	14.83 ± 1.26	16.05 ± 2.00	4.96 ± 0.32
3a	5.13 ± 0.35	8.97 ± 0.64	1.94 ± 0.12
4a	0.049 ± 0.005	0.056 ± 0.01	0.012 ± 0.005
1b	0.21 ± 0.02	1.49 ± 0.10	0.13 ± 0.01
2b	4.23 ± 0.30	6.55 ± 0.57	2.88 ± 0.18
Cisplatin	2.89 ± 0.34	6.48 ± 0.81	2.65 ± 0.33

Previously, we reported the synthesis and antitumor activity of a mixed-ligand complex di-n-butyl-(4-chlorobenzohydroxamate) tin(IV) chloride (DBDCT) [27], which exhibited strong *in vitro* cytotoxic activity toward HL-60 (IC_{50} > 1.0 μM), SGC-7901 (IC_{50} = 0.081 μM), Hela (IC_{50} > 10 μM) and T24 (IC_{50} > 1.0 μM) cell lines. The difference between **4a** and DBDCT is defined by the type and position of the X substituent. For example, comparison of the IC_{50} values suggests that compound **4a** with two fluorine atoms is better than the DBDCT with one chlorine atom. Indeed, the amount and position of X-substituents tend to affect greatly the antitumor activity. The inhibitory potencies of the compounds may be correlated with the hydrophobic properties (for **4a**, clog*P* = 5.109, but for DBDCT, clog*P* = 5.536).

2.5. Annexin V FITC-PI assay of apoptosis cells

On the basis of the cytotoxicity effect study, compounds **1b** and **4a** with good activities were selected for further examinations to determine the apoptosis rate of tumor cells. Since KB cells appeared to be the most sensitive ones to the tested compounds, we carried out this study in KB cells.

Early stages of apoptosis are characterized by perturbations in the cellular membrane. It leads to a redistribution of phosphatidylserine (PS) to the external side of the cell membrane, which causes a Ca flux. Annexin V is a Ca-dependent phospholipid-binding protein with high affinity for PS. Therefore, fluorescently labeled annexin V can be used to identify early apoptosis cells. Late apoptosis and necrotic cells have lost membrane integrity, and can be stained by propidium iodide (PI). The percentage of apoptosis was presented in Table 2 and Fig. 3 by the region Q4 (early apoptosis) and Q2 (late apoptosis and necrotic cell) and total percentages of apoptosis.

Although negative control cells induced little apoptosis (ca. 21.2%), the percentages of apoptotic cells treated with compounds

Table 2
The percentages of apoptosis of **4a** and **1b** in different concentrations with cisplatin as positive control.

Complex	Concentration (μM)	Q2 (late apoptosis and necrotic cell)	Q4 (early apoptosis)	Total percentage
Control		5.4	15.8	21.2
4a	2.5	28.6	26.2	54.8
	10	58.8	26.0	84.8
	20	66.5	17.4	83.9
1b	2.5	7.9	9.8	17.7
	10	18.1	38.1	56.2
	20	13.7	23	36.7
cisplatin	2.5	7.4	8.6	16.0
	10	10.2	8.0	18.2
	20	7.0	9.0	16.0

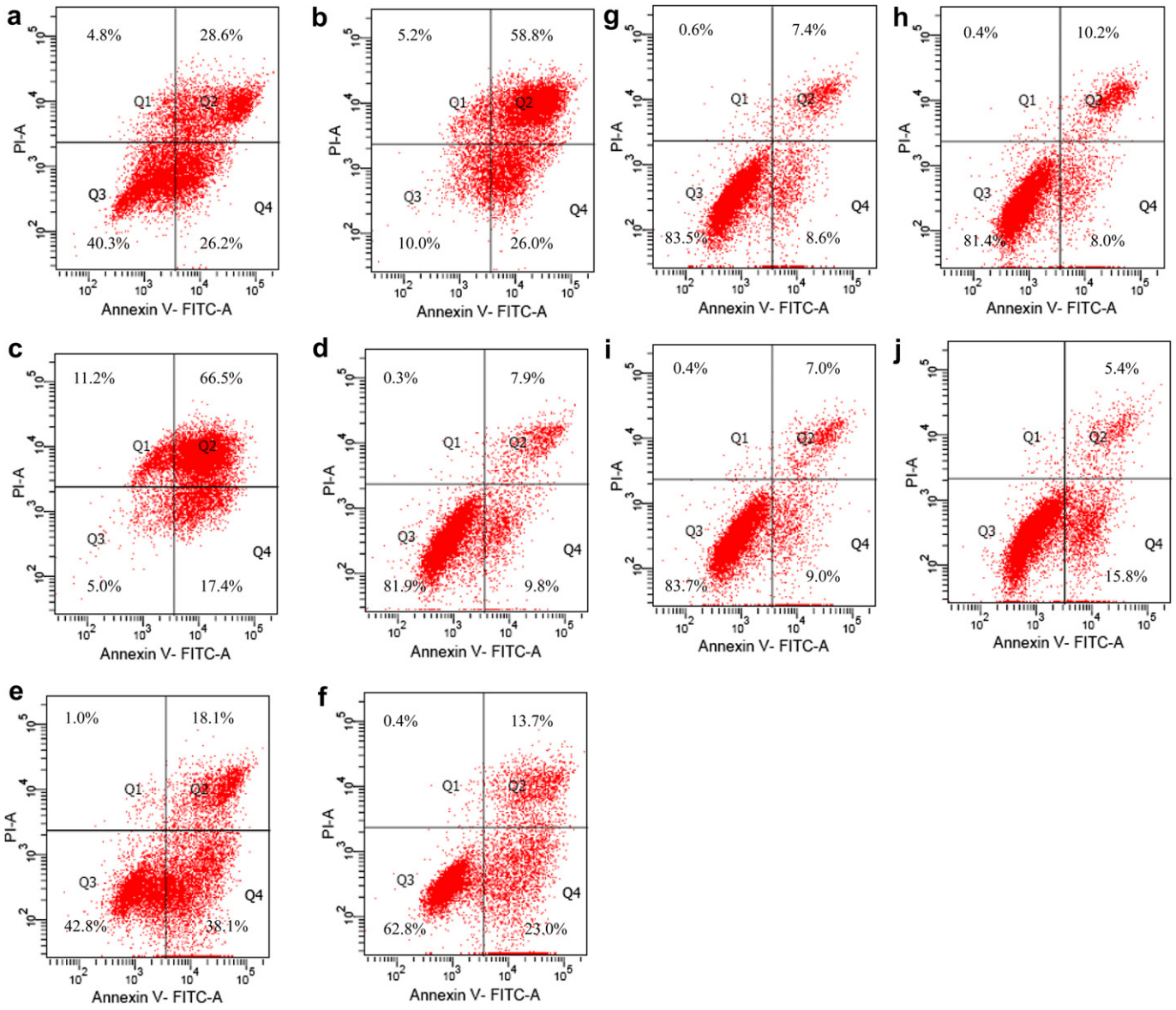

Fig. 3. Apoptosis detection in KB cells using the Annexin V assay after 24 h. The total percentage of apoptotic cells was considered as Q2 + Q4. Plot presents the fluorescence data of propidium iodide (PI) and Annexin V fluorescein corresponding to (a) 54.8% (2.5 μM, **4a**), (b) 84.8% (10.0 μM, **4a**), (c) 83.9% (20 μM, **4a**), (d) 17.7% (2.5 μM, **1b**), (e) 56.2% (10 μM, **1b**), (f) 36.7% (20 μM, **1b**), (g) 16.0% (2.5 μM, Cisplatin), (h) 18.2% (10 μM, Cisplatin), (i) 16.0% (20 μM, Cisplatin), (j) 21.2% (control) apoptotic cells.

1b or **4a** were significantly greater (>56.2% in 10 μM) than those of control cells. For **4a**, the total apoptosis percentage is 54.8, 84.8 and 83.9% at the concentration of 2.5, 10 and 20 μM, respectively. For **1b**, the total apoptosis percentage is 17.7, 56.2 and 36.7% at the concentration of 2.5, 10 and 20 μM, respectively. Both complexes **1b** and **4a** were significantly more toxic than cisplatin to KB cells, which even at concentration of 20 μM did not show obvious toxicity. This enhanced antitumor effect was possibly due to the improved lipophilicity of **1b** and **4a**. These data demonstrated again the cytotoxicity of both **1b** and **4a**, and compound **4a** was even better than compound **1b**, consistent with the former cytotoxicity assays.

Apoptosis is an orderly process designed to remove unwanted cells; it can also be triggered by damage to the cell. Necrosis is a disordered process. Although apoptosis and necrosis are conceptually distinct forms of cell death with very different morphological and biochemical characteristics, these two types of demise may occur simultaneously in tissues or cell cultures exposed to the same insult [34]. Moreover, depending on different dose of drug and cellular status, the mechanism of cell death induced by drugs may different. From the Annexin V FITC-PI assay, it is hard to differentiate the late apoptosis cells and necrosis cells. The conditions under which the apoptotic program is induced by **1b** and **4a** will be studied further.

2.6. Cell cycle distribution analysis by flow cytometry

Cell cycle analysis was performed to investigate the anti-proliferative effects of the two complexes of **1b** and **4a**. Differentiation between phases of the cell cycle is based on the content of genetic material, which in non-dividing cells is limited to one copy of DNA. The cell population in the S phase (DNA replication phase) is synthesizing genetic material, and thus contains more DNA than quiescent cells. The subsequent G_2/M phase (interphase/mitosis) is characterized by the presence of two copies of DNA. Therefore, the alternations in these phases were used as a basis for the comparison of different treatments.

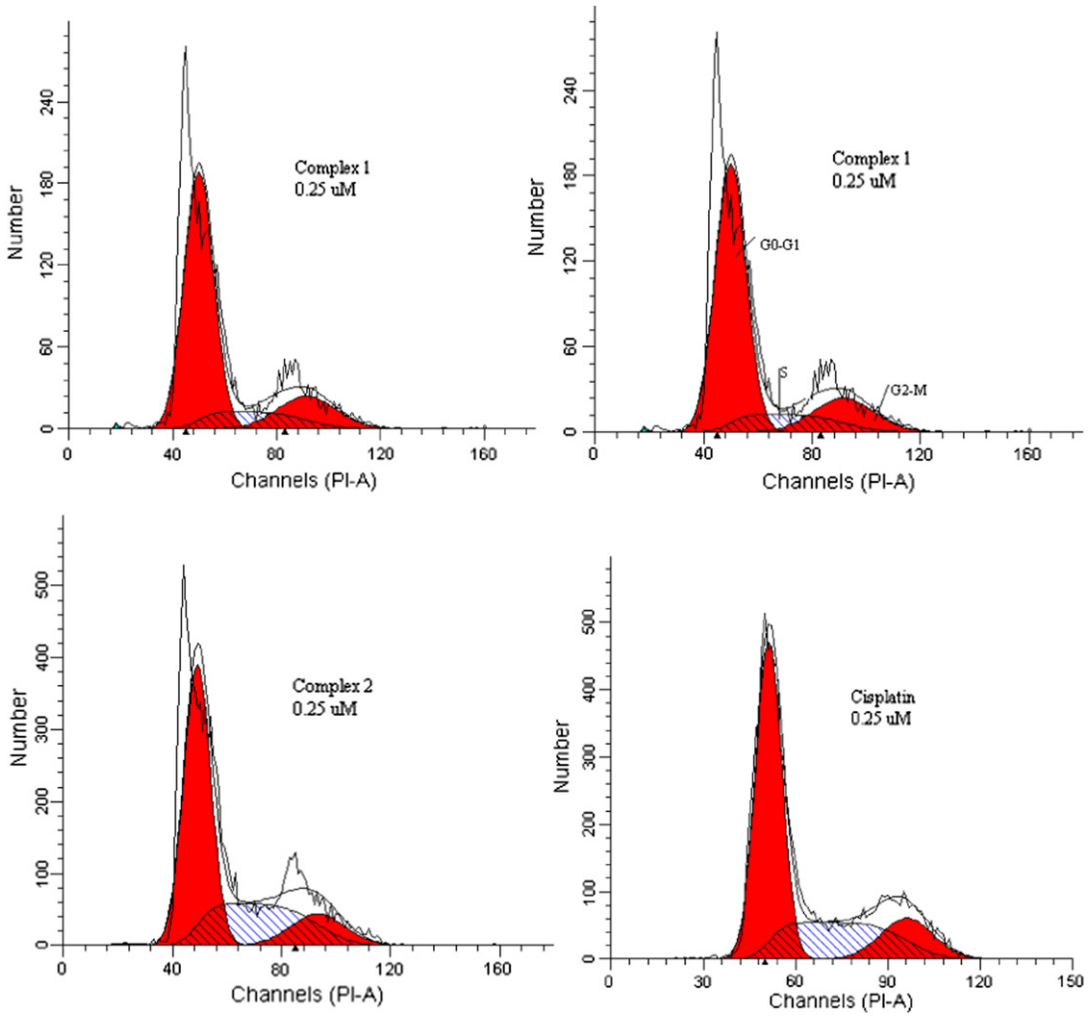

Fig. 4. Flow cytometric analysis on the cell cycle distribution of KB cells after treatment with **4a**, **1b** and cisplatin. G_0-G_1: first-growth phase, S: DNA-synthesis phase, G_2-M: second-growth phase and mitotic phase.

In order to study DNA cell content changes in cell cycle, cell cycle analysis was performed by PI single labeling (Fig. 4). The concentrations of drugs were decreased to 0.25, 0.5 and 1 μM, without causing cell apoptosis. From the Table 3, cells exposure to **1b**, **4a** and cisplatin all led to a decrease in the percentages of S phase, and an increase in the percentage of G_0/G_1 phase. Compound **4a** showed a much stronger antitumor effect and led to higher cells arrest at G_0/G_1 phases than **1b** and cisplatin.

3. Conclusions

Both **1b** and **4a** exhibited strong *in vitro* cytotoxic activities toward the tested three human tumor cell lines HL-60, BGC-823 and KB, and they were higher than cisplatin. Among the three cell lines, KB cells appeared to be the most sensitive to these organotin(IV) complexes. KB cell apoptosis-induced by **1b** or **4a** was examined by flow cytometric analysis, staining assays with propidium iodide and annexin V FITC; the results indicated that both of the organotin(IV) derivatives were able to induce the apoptosis. Cancer cell cycles were effectively blocked at G_0–G_1 and G_2–M phase at low concentration of two tin(IV) complexes. Complex **4a** has been shown to be a more potent antitumor agent and to have a higher apoptosis-induced effect than either complex **1b** or cisplatin, which is consistent with the compounds cytotoxic effects. Currently, studies are ongoing in our laboratory in order to gain a better insight into the biochemical mechanism of antitumor action of these tin(IV) compounds, which may be beneficial in the design of new metal-based antitumor agents.

Table 3
Cell populations of KB cells after treating by two tin(IV) complexes.

Complex	Concentration (μM)	G_0/G_1 (%)	G_2/M (%)	S (%)
Control		50.73	7.25	42.02
4a	0.25	68.65	17.34	14.01
1b	0.25	57.06	12.75	30.19
	0.5	59.29	3.89	36.82
	1	67.45	10.16	22.38
cisplatin	0.25	57.37	14.77	27.86
	0.5	51.72	13.01	35.27
	1	52.52	12.96	34.52

4. Experimental

4.1. Materials and physical measurements

Di-n-butyltin(IV) dichloride was purchased from Aldrich and used as received. The other reagents were of analytical grade. The ligands were prepared according to the previous methods [16]. Elemental analyses were performed on PE-2400-II elemental

Table 4
Experimental data for crystallographic analyses for complexes **4a** and **1b**.

	4a	**1b**
Chemical formula	$C_{15}H_{22}ClF_2NO_2Sn$	$C_{74}H_{100}Br_6N_6O_{12}Sn_4$
M (g mol^{-1})	440.48	2219.82
Crystal system	Monoclinic	Triclinic
Space group	$P2(1)/m$	$P-1$
a (Å)	5.0140(17)	11.0967(4)
b (Å)	21.301(7)	13.6572(3)
c (Å)	17.602(6)	16.1020(4)
α (°)	90	69.639(2)
β (°)	98.19	70.922(2)
γ (°)	90	86.641(2)
Volume(Å^3)	1860.8(11)	2157.94(11)
Z	4	1
ρ_{calc} (g cm^{-3})	1.572	1.708
μ (mm^{-1})	1.540	3.979
Reflections collected	18001	15790
Individual reflections [R(int)]	3738 [0.1117]	8792 [0.1257]
θ completeness [%]	26.00° [99.3]	26.50°[98.2]
h.k.l range	$-6 \le h \le 6$	$-13 \le h \le 13$
	$-26 \le k \le 24$	$-14 \le k \le 17$
	$-21 \le l \le 21$	$-13 \le l \le 20$
Data/restrictions/parameters	3738/22/407	8792/10/464
GOF on F^2	1.069	0.873
Final indices [$I > \sigma(I)$]	$R_1 = 0.0581$	$R_1 = 0.0657$
	$wR_2 = 0.1567$	$wR_2 = 0.1470$
Final indices (all data)	$R_1 = 0.0675$	$R_1 = 0.1222$
	$wR_2 = 0.1657$	$wR_2 = 0.1805$

analyzer. IR spectra in the range 4000–400 cm^{-1} were recorded on Perkin–Elmer one FT-IR spectrophotometer with samples investigated as KBr discs. ^{1}H, ^{13}C, ^{119}Sn NMR spectra were recorded on a Varian INOVA 600 spectrometer (600.0 MHz for ^{1}H, 150.8 MHz for ^{13}C, 223.6 MHz for ^{119}Sn) at ambient temperature [δ values in ppm relative to Me_4Si (^{1}H, ^{13}C) or Me_4Sn (^{119}Sn)].

4.2. Synthesis of [^{n}Bu$_2$Sn{3,4-F$_2$C$_6$H$_3$(C=O)NHO}Cl] (**1a**)

Di-n-butyltin(IV) dichloride (0.151 g, 0.5 mmol) was added to an anhydrous methanol solution (10 mL) of 3,4-difluorobenzohydroxamic acid (0.086 g, 0.5 mmol) and potassium hydroxide (0.028 g, 0.5 mmol). The solution was stirred under N_2 at room temperature overnight. Water (10 mL) was then added leading to the formation of a white precipitate, which was then separated by filtration, recrystallized from methanol, and colorless needle-shaped crystals of **1a** were slowly formed at room temperature. Yield: 33%. Anal. Calc. for $C_{15}H_{22}ClF_2NO_2Sn$ (440.48): C 40.90, H 5.03, N 3.18. Found C 40.99, H 4.92, N 3.15. IR: ν = 3232 s (N–H); 1602 s (C'O)/(N'C); 908 s (N–O); 536 m (Sn–C); 420 s (Sn–O) cm^{-1}. ^{1}H NMR ($CDCl_3$): δ = 11.05 (br, 1H, NH), 7.64–7.45 (m, 3H, C_6H_3), 1.75–1.62 (m, 8H, 2CH$^2_2$CH$^1_2$), 1.41–1.35 (m, 4H, 2C^{3}H$_2$), 0.86 (t, J = 7.2 Hz, 6H, 2C^{4}H$_3$) ppm. ^{13}C NMR ($CDCl_3$): δ = 160.1 (CO), 149.0, 132.3, 129.4, 117.5 and 113.4 (C_{arom}), 27.3 (CH$^1_2$, R–Sn) and 26.5 (CH$^1_2$, R–Sn), 26.3, 24.8, 13.3 (R–Sn) ppm. ^{119}Sn NMR ($CDCl_3$): δ = −62.0 ppm.

4.3. Synthesis of [^{n}Bu$_2$Sn{2,4-F$_2$C$_6$H$_3$(C=O)NHO}Cl] (**2a**)

Compound **2a** was prepared by following the method and conditions described for **1a** and using 2,4-difluorobenzohydroxamic acid (0.086 g, 0.5 mmol). The white product was recrystallized from methanol and dried in vacuo. Yield: 38%. Anal. Calc. for $C_{15}H_{22}ClF_2NO_2Sn$ (440.48): C 40.90, H 5.03, N 3.18. Found C 40.76, H 5.11, N 3.10. IR: ν = 3226 s (N–H); 1616 s (C'O)/(N'C); 901 s (N–O); 522 m (Sn–C); 418 s (Sn-O) cm^{-1}. ^{1}H NMR ($CDCl_3$): δ = 10.02 (br, 1H, NH), 7.78–6.88 (m, 3H, C_6H_3), 1.72–1.65 (m, 8H, 2CH$^2_2$CH$^1_2$), 1.41–1.37 (m, 4H, 2C^{3}H$_2$), 0.91 (t, J = 7.2 Hz, 6H, 2C^{4}H$_3$) ppm. ^{13}C NMR ($CDCl_3$): δ = 165.2 (CO), 157.6, 152.4, 127.8, 124.3, 120.0, 117.2 (C_{arom}), 28.1 (CH$^1_2$, R–Sn) and 27.4 (CH$^1_2$, R–Sn), 26.8, 13.5 (R–Sn) ppm. ^{119}Sn NMR ($CDCl_3$): δ = −67.5 ppm.

4.4. Synthesis of [^{n}Bu$_2$Sn{2,5-F$_2$C$_6$H$_3$(C=O)NHO}Cl] (**3a**)

Compound **3a** was prepared by following the method and conditions described for **1a** and using 2,5-difluorobenzohydroxamic acid (0.086 g, 0.5 mmol). The white product was recrystallized from methanol and dried in vacuo. Yield: 55%. Anal. Calc. for $C_{15}H_{22}ClF_2NO_2Sn$ (440.48): C 40.90, H 5.03, N 3.18. Found C 40.80, H 5.15, N 3.12. IR: ν = 3227 s (N–H); 1610 s (C'O)/(N'C); 898 s (N–O); 518 m (Sn–C); 421 s (Sn–O) cm^{-1}. ^{1}H NMR ($CDCl_3$): δ = 7.64–7.21 (m, 3H, C_6H_3), 1.67–1.56 (m, 8H, 2CH$^2_2$CH$^1_2$), 1.37–1.25 (m, 4H, 2C^{3}H$_2$), 0.90 (t, J = 7.2 Hz, 6H, 2C^{4}H$_3$) ppm. ^{13}C NMR ($CDCl_3$): δ = 159.4 (CO), 154.6, 152.4, 132.8, 122.5, 117.4, 104.7(C_{arom}), 27.8 (CH$^1_2$, R–Sn) and 26.7 (CH$^1_2$, R–Sn), 25.9, 13.5 (R–Sn) ppm. ^{119}Sn NMR ($CDCl_3$): δ = −61.4 ppm.

4.5. Synthesis of [^{n}Bu$_2$Sn{2,6-F$_2$C$_6$H$_3$(C=O)NHO}Cl] (**4a**)

Compound **4a** was prepared by following the method and conditions described for **1a** and using 2,6-difluorobenzohydroxamic acid (0.086 g, 0.5 mmol). The white product was recrystallized from methanol and dried in vacuo. Yield: 41%. Anal. Calc. for $C_{15}H_{22}ClF_2NO_2Sn$ (440.48): C 40.90, H 5.03, N 3.18. Found C 40.51, H 5.14, N 3.13. IR: ν = 3234 s (N–H); 1627 s (C'O)/(N'C); 879 s (N–O); 514 m (Sn–C); 417 s (Sn–O) cm^{-1}. ^{1}H NMR ($CDCl_3$): δ = 10.09 (s, br, 1H, NH), 7.51–7.49 (m, br, 1H, H(4), C_6H_3), 7.05–7.02 (m, br, 2H, H(3,5), C_6H_3), 1.78–1.60 (m, 8H, 2CH$^2_2$CH$^1_2$), 1.43–1.25 (m, 4H, 2C^{3}H$_2$), 0.93 (t, J = 7.2 Hz, 6H, 2C^{4}H$_3$) ppm. ^{13}C NMR ($CDCl_3$): δ = 161.6 (CO), 159.0, 157.4, 133.8, 112.6 and 112.4 (C_{arom}), 27.5 (CH$^1_2$, R–Sn) and 26.8 (CH$^1_2$, R–Sn), 26.6, 26.3, 25.9, 13.6 (R–Sn) ppm. ^{119}Sn NMR ($CDCl_3$): δ = −60.3 ppm.

4.6. Synthesis of [^{n}Bu$_4$Sn$_2${(3-Br)C$_6$H$_4$C(=O)NHO}$_2${(3-Br)C$_6$H$_4$C(=NO)O}]$_2$ (**1b**)

Di-n-butyltin(IV) dichloride (0.151 g, 0.5 mmol) was added dropwise to an anhydrous methanolic solution (15 ml) of 3-bromobenzohydroxamic acid (0.215 g, 1.0 mmol) and KOH (0.056 g, 1.0 mmol). The solution was stirred under N_2 at room temperature overnight. Water (15 ml) was added to form a white precipitate, which was separated by filtration, washed with water and cold methanol. The white solid was then recrystallized from n-heptane. Colorless block-shaped crystals of **1b** were slowly formed at room temperature. Yield: 27%. Anal. Calcd for $C_{74}H_{100}Br_6N_6O_{12}Sn_4$ (2219.82): C, 40.04; H, 4.54; N, 3.79. Found: C, 39.62; H, 4.61; N, 3.65. IR: ν = 3297, 1616, 1561, 1162, 722, 672, 524, 464 cm^{-1} ^{1}H NMR ($CDCl_3$): δ = 7.84–7.15 (m, br, 12H, 3C$_6$H$_4$), 1.88–1.63 (m, br, CH$^2_2$CH$^1_2$), 1.43–1.28 (m, br, C^{3}H$_2$), 0.81(m, br, CH$_3$) ppm. ^{13}C NMR ($CDCl_3$): δ = 161.9, 161.2, 154.0, 134.6, 130.1, 129.8, 125.0, 122.7, 29.6, 27.3, 26.0, 25.0, 13.6 ppm ^{119}Sn NMR ($CDCl_3$): δ = −267.4, −269.7, −273.0, −279.8 ppm.

4.7. Synthesis of [^{n}Bu$_4$Sn$_2${(4-Br)C$_6$H$_4$C(=O)NHO}$_2${(4-Br)C$_6$H$_4$C(=NO)O}]$_2$ (**2b**)

Compound **2b** was prepared by following the method and conditions described for **1b** and using 4-bromobenzohydroxamic acid (0.215 g, 1.0 mmol). The white solid was then recrystallized from n-heptane and dried in vacuo. Yield: 56%. Anal. Calc. for $C_{15}H_{22}ClF_2NO_2Sn$ (440.48): C 40.90, H 5.03, N 3.18. Found C 40.78, H 5.11, N 3.12. IR: ν = 3288, 1614, 1556, 901, 578, 468 cm^{-1} ^{1}H NMR

($CDCl_3$): δ = 7.78–7.04 (m, br, 12H, $3C_6H_4$), 1.77–1.62 (m, br, $CH^2{}_2CH^1{}_2$), 1.38–1.34(m, br, C^3H_2), 0.88 (m, br, CH_3) ppm. ^{13}C NMR ($CDCl_3$): δ = 163.5, 162.1, 161.9, 159.9, 131.8, 128.7, 126.8, 124.1, 118.4, 113.7, 112.8, 28.6, 27.5, 26.7, 23.3, 13.8 ppm ^{119}Sn NMR ($CDCl_3$): δ = −213.2, −214.9, −215.3, −215.7 ppm.

4.8. X-ray crystallography

Suitable single crystals of the complexes were mounted in glass capillaries for X-ray structural analysis. Diffraction data were collected on a Bruker SMART CCD diffractometer with Mo Kα (λ = 0.71073 Å) radiation at room temperature (298 K). Crystallographic details are reported in Table 4. During the intensity data collection, no significant decay was observed. The intensities were collected for Lorentz-polarization effects and empirical absorption with the SADABS program. The structures were solved by direct methods using the SHELXL-97 program. All non-hydrogen atoms were found from the difference Fourier syntheses. The H atoms were included in calculated positions with isotropic thermal parameters related to those of the supporting carbon atoms but were not included in the refinement. All calculations were performed using the Bruker Smart program [35].

4.9. In vitro cytotoxic activity

The following cell lines were used for screening: human promyelocytic leukemic (HL-60), human gastric carcinoma (BGC-823), and human nasopharyngeal carcinoma (KB) cell lines. All of them were grown and maintained in RPMI-1640 medium supplemented with 10% fetal bovine serum, penicillin (100 U/mL), and streptomycin (100 μg/mL) at 37 °C in humidified incubators in an atmosphere of 5% CO_2.

The complexes were dissolved in DMSO at a concentration of 5 mM as stock solution, and diluted in culture medium at concentrations of 1.0, 10, 100, and 500 mM as working-solution. To avoid DMSO toxicity, the concentration of DMSO was less than 0.1% (v/v) in all experiments.

The cells harvested from exponential phase were seeded equivalently into a 96-well plate, and then the complexes were added to the wells to achieve final concentrations. Control wells were prepared by addition of culture medium. Wells containing culture medium without cells were used as blanks. All experiments were performed in quintuplicate. The MTT assay was performed as described by Mosmann for HL-60 [36]. Upon completion of the incubation for 48 h, stock MTT dye solution (20 μl, 5 mg/ml) was added to each well. After 4 h incubation, 2-propanol (100 μl) was added to solubilize the MTT formazan. The OD of each well was measured on a microplate spectrophotometer at a wavelength of 570 nm. The SRB assay was performed as previously described for BGC-823 and KB [37]. Upon completion of the incubation for 48 h, the cells were fixed in 10% trichloroacetic acid (100 μl) for 30 min at 4 °C, washed five times and stained with 0.1% SRB in 1% acetic acid (100 μl) for 15 min.The cells were washed four times in 1% acetic acid and air-dried. The stain was solubilized in 10 mM unbuffered Tris base (100 μl) and OD was measured at 540 nm as above. The IC_{50} value was determined from plot of % viability against dose of compounds added.

4.10. Cell apoptosis assay

KB Cells were seeded in sterile six-well plates at a density of 1×10^6 and grown in 5% CO_2 at 37 °C. After 24 h incubation, cells were exposed to **1b**, **4a** and cisplatin for 24 h at concentrations of 2.5 μM, 10 μM, 20 μM. Then the drugs were washed by cold PBS and harvested by trysinisation and collected by centrifugation and washed two times with PBS. Re-suspended cells in 500 μl binding buffer and added 5 μl of Annexin V-FITC and 10 μl of PI to cells, and then cells were incubated for 30 min at 4 °C in the dark and then analyzed by flow cytometry (BD-LSR II flow cytometry).

4.11. Cell cycle analysis

Cells were seeded in sterile six-well plates at a density of 1×10^6 and grown in 5% CO_2 at 37 °C. After 24 h incubation, cells were exposed to **1b**, **4a** and cisplatin for 24 h at concentrations of 0.25 μM, 0.5 μM, 1 μM. Then the drugs were washed by cold PBS and harvested by trysinisation and collected by centrifugation and washed two times with PBS. Re-suspended cells in 300 μL cold PBS and added dropwise 700 μL ethanol. After the cells were fixed at −20 °C overnight, the cells were centrifuged and re-suspended in PBS for 5 min. Then the cells were harvested by centrifugation. 100 μL RNase A were added, and cells were incubated with it for 30 min at 37 °C. After that, 100 μL (100 μg/ml) PI were added and cells were incubated with is for 30 min at 4 °C in the dark and then detected by flow cytometry (BD-LSR II low cytometry) and analyzed by ModFit software.

Acknowledgments

This work has been partially supported by the National Natural Science Foundation of China (No: 81102311), the Science and Technology Department of Hubei Province of China (No: 2008CDB242), the Fundamental Research Funds for the Central Universities and Huazhong University of Science and Technology (No: 2011QN242).

Supplementary material

CCDC-844678 (**4a**) and 844679 (**1b**) contain the supplementary crystallographic data for this paper. These data can be obtained free of charge via www.ccdc.cam.ac.uk/data_request/cif or by emailing data_request@ccdc.cam.ac.uk or by contacting The Cambridge Crystallographic Data Centre, 12, Union Road, Cambridge, CB2 1EZ, UK; fax: +441223 336033.

Appendix. Supplementary material

Supplementary data related to this article can be found online at doi:10.1016/j.ejmech.2011.12.032.

References

[1] S.K. Hadjikakou, N. Hadjiliadis, Coord. Chem. Rev. 253 (2009) 235–249.
[2] M. Gielen, Coord. Chem. Rev. 151 (1996) 41–51.
[3] M. Gielen, E.R.T. Tiekink (Eds.), Metallotherapeutic Drug and Metal-Based Diagnostic Agents: 50Sn Tin Complexes and Their Therapeutic Potential, Wiley, New York, 2005.
[4] M. Gielen, Appl. Organomet. Chem. 16 (2002) 481–494.
[5] E.R. Tiekink, M. Gielen, Metallotherapeutic Drugs and Metal-Based Diagnostic Agents: The Use of Metals in Medicine, John Wiley & Sons Ltd, The Atrium, Southern gate, Chichester, West Sussex PO19 8SQ, England, 2005, 421–435.
[6] J.C. Michael, Z. Fuchun, R.F. Dominic, Chem. Rev. 99 (1999) 2511–2533.
[7] L. Pellerito, L. Nagy, Coord. Chem. Rev. 224 (2002) 111–150.
[8] C. Pellerito, L. Nagy, L. Pellerito, A. Szorcsik, J. Organomet. Chem. 691 (2006) 1733–1747.
[9] S. Tabassum, C. Pettinari, J. Organomet. Chem. 691 (2006) 1761–1766.
[10] X. Shang, X. Meng, E.C.B.A. Alegria, Q. Li, M.F.C. Guedes da Silva, M.L. Kuznetsov, A.J.L. Pombeiro, Inorg. Chem. 50 (2011) 8158–8167.
[11] S.K. Choudhuri, S. Das Dutta, R. Chatterjee, J.R. Chowdhury, Chemotherapy 37 (1991) 122–127.
[12] V.S. Petrosyan, N.S. Yashina, S.V. Ponomarev, Metal-Based Drugs 5 (1998) 237–244.
[13] Q. Li, M.F.C. Guedes da Silva, A.J.L. Pombeiro, Chem. Eur. J. 10 (2004) 1456–1462.

[14] Q.S. Li, M.F.C. Guedes da Silva, J.H. Zhao, A.J.L. Pombeiro, J. Organomet. Chem. 689 (2004) 4584–4591.
[15] X.M. Shang, Q.S. Li, J.Z. Wu, J. Organomet. Chem. 690 (2005) 3997–4000.
[16] X.M. Shang, J.Z. Wu, Q.S. Li, Eur. J. Inorg. Chem. (2006) 4143–4150.
[17] X.M. Shang, J.Z. Wu, A.J.L. Pombeiro, Q.S. Li, Appl. Organomet. Chem. 21 (2007) 919–925.
[18] X.M. Shang, J.R. Cui, J.Z. Wu, A.J.L. Pombeiro, Q.S. Li, J. Inorg. Biochem. 102 (2008) 901–909.
[19] M. Gajewska, K.V. Luzyanin, M.F.C. Guedes da Silva, Q. Li, J. Cui, A.J.L. Pombeiro, Eur. J. Inorg. Chem. 25 (2009) 3765–3769.
[20] A. Jancso, L. Nagy, E. Moldrheim, E. Sletten, J. Chem. Soc. Dalton Trans. (1999) 1587–1594.
[21] Q. Li, P. Yang, H. Wang, M. Guo, J. Inorg. Biochem. 64 (1996) 181–195.
[22] R. Barbieri, A. Silvestri, A.M. Giuliani, V. Piro, F. Di Simone, G. Madonia, J. Chem. Soc. Dalton Trans. (1992) 585–590.
[23] X.M. Shang, J.Z. Wu, Q.S. Li, Chin. J. Chem. 26 (2008) 627–630.
[24] F.J. Ramos-Lima, A.G. Quiroga, B. García-Serrelde, F. Blanco, A. Carnero, C. Navarro-Ranninger, J. Med. Chem. 50 (2007) 2194–2199.
[25] Y.J. Liu, C.H. Zeng, Z.H. Liang, J.H. Yao, H.L. Huang, Z.Z. Li, F.H. Wu, Eur. J. Med. Chem. 45 (2010) 3087–3095.
[26] C. Tan, S. Lai, S. Wu, S. Hu, L. Zhou, Y. Chen, M. Wang, Y. Zhu, W. Lian, W. Peng, L. Ji, A. Xu, J. Med. Chem. 53 (2010) 7613–7624.
[27] Y. Li, L. Yang, X. Liu, J. Liu, X. Shang, J. Guo, Q. Li, Inorg. Biochem. 102 (2008) 1731–1735.
[28] M.K. Das, S.J. De, J. Organomet. Chem. 495 (1995) 177–184.
[29] M.K. Das, P. Bose, N. Roy, J. Chem. Eng. Data 29 (1984) 345–351.
[30] J. Holceek, M. Nadvornik, K. Handlir, A. Lvcka, J. Organomet. Chem. 315 (1986) 299–308.
[31] J. Otera, J. Organomet. Chem. 221 (1981) 57–61.
[32] P.G. Harrison, T.J. King, R.C. Phillips, J. Chem. Soc. Dalton Trans. (1976) 2317–2321.
[33] P.G. Harrison, T.J. King, J.A. Richards, J. Chem. Soc. Dalton Trans. (1975) 826–830.
[34] V.M. Gonzalez, M.A. Fuertes, C. Alonso, J.M. Perez, Mol. Pharmacol. 59 (2001) 657–663.
[35] G.M. Sheldrick, SHELXTL-97, Program for X-ray Crystal Structure Solution and Refinement, Göttingen University, Germany, 1997.
[36] T. Mosmann, J. Immunol. Methods 65 (1983) 55–63.
[37] P. Skehan, R. Storeng, D. Scudiero, A. Monks, J. McMahon, D. Vistica, J.T. Warren, H. Bokesch, S. Kenney, M.R. Boyd, J. Natl. Cancer Inst. 82 (1990) 1107–1112.